applied sciences

MDPI

Article

Mechatronics Design of a Gait-Assistance Exoskeleton for Therapy of Children with Duchenne Muscular Dystrophy

Jaime Arcos-Legarda [1], David Torres [2], Fredy Velez [2], Hernan Rodríguez [2], Alexander Parra [2] and Álvaro Gutiérrez [1,*]

[1] Escuela Técnica Superior de Ingenieros de Telecomunicación, Universidad Politécnica de Madrid, 28040 Madrid, Spain
[2] Department of Mechatronics Engineering, Universidad de San Buenaventura, Bogotá 110141, Colombia
* Correspondence: a.gutierrez@upm.es

Abstract: This paper presents a mechatronics design of a gait-assistance exoskeleton for therapy in children with Duchenne muscular dystrophy (DMD). This type of muscular dystrophy is a severe condition that causes muscle wasting, which results in a progressive loss of mobility. Clinical studies have shown the benefits of physical therapy in prolonging the mobility of patients with DMD. However, the therapy sessions are exhaustive activities executed by highly qualified rehabilitation personnel, which makes providing appropriate treatment for every patient difficult. This paper develops a mechatronics design of a gait-assistance exoskeleton to automate therapy sessions. The exoskeleton design uses adaptable mechanisms to adjust the device to the patient's needs and includes the design of a series-elastic actuator to reduce the effects of nonalignment of the rotation axis between the exoskeleton and the patient. A mathematical dynamic hybrid model of the exoskeleton and a child's body is developed using anthropometry of a population of six-year-old children. The hybrid model is used to design a nonlinear control strategy, which uses differential geometry to perform feedback linearization and to guarantee stable reference tracking. The proposed control law is numerically validated in a simulation to evaluate the control system's performance and robustness under parameter variation during therapy with trajectory-tracking routines.

Keywords: gait exoskeleton; wearable robots; biomechatronics; mechatronics design; Duchenne muscular dystrophy

check for updates

Citation: Arcos-Legarda, J.; Torres, D.; Velez, F.; Rodríguez, H.; Parra, A.; Gutiérrez, A. Mechatronics Design of a Gait-Assistance Exoskeleton for Therapy of Children with Duchenne Muscular Dystrophy. *Appl. Sci.* **2023**, *13*, 839. https://doi.org/10.3390/app13020839

Academic Editor: Shin-Da Lee

Received: 9 December 2022
Revised: 30 December 2022
Accepted: 5 January 2023
Published: 7 January 2023

1. Introduction

Duchenne muscular dystrophy (DMD) is a disease that affects approximately 4.78 per 100.000 born male children [1,2]. DMD is produced by an X-linked recessive dystrophy myopathy caused by the absence of *dystrophin proteins* in the muscular system, myocardium, and brain [3]. This pathology is characterized by muscular weakness that leads to early confinement in a wheelchair. Several complications may arise during the course of the disease such as irregular muscle fatigue, lack of stability during walking, and cardiac and respiratory complications, especially during adult ages [4]. A few years ago, DMD was considered a disease with zero treatment expectations; however, nowadays, there are methods used to slow down the natural evolution of the disease through early diagnosis and specialized treatments. These treatments include the use of corticosteroids such as prednisona and deflazacort [5], as well as gene and stem cells therapy [6]. One of the most effective treatments to slow down the muscular dystrophy evolution is physical therapy with muscular stretching and nutritional supplements to maintain symmetrical muscle mobility [7].

Physical therapy for individuals with DMD has been shown to be helpful in monitoring changes in strength, range of motion, and functional mobility. Additionally, it provides a tool for interventions in and education of individuals and their families on stretching, positioning, and activity pacing [8]. Nevertheless, providing constant and reliable therapy is a complex task due to the limited access to rehabilitation centers. This is a common problem for illnesses that require physical therapy. Nowadays, progress has been made to tackle this problem with an engineering perspective using exoskeletons to assist movement that improves functional walking ability [9]; however, the development of such tools for the treatment of DMD patients has been scarce. Applications of wearable arm exoskeletons have been developed for assisting patients with DMD and help them to improve their performance in the execution of daily life activities [10]. These applications allow for enhancing upper extremity function of DMD patients via robotic exoskeletons [11–13] However, less attention has been devoted to the development of exoskeletons for lower limb assistance or therapy.

Consensus on the treatment of patients with DMD has pointed out that appropriate physical therapy could reduce the rate of progression of the disease [7]. These treatments should be formulated by a multidisciplinary team including neurologists, pediatrics, neurologists, and rehabilitators, which should adapt the therapy to the patient's stage of clinical progression. However, performing physical therapy according to medical recommendations could be challenging due to the lack of appropriate technological tools. The aims of treatment during the early DMD phases are devoted to maintaining a level of activities that preserves the ability to perform daily functions. In this way, to maintain muscle strength, the use of orthopedic devices such as knee–ankle–foot orthoses (KAFOs) could prolong the patients' independence and mobility [14]. The early stages of DMD are focused on preserving muscle extensibility and joint mobility and symmetry to prevent contractures and deformities [15]. To accomplish the objective of maintaining the muscles and joints' functionality, each patient should receive between four to six sessions of physical therapy per week [16]. However, achieving this high frequency of therapy is not feasible because of the limited medical personnel available at these therapy centers. This reveals the need for the development of technological tools that allow for preventive management of muscle flexibility and extensibility.

Gait exoskeletons have been used to assist therapy of children that suffer cerebral paralysis [17] and spinal muscular atrophy. Atlas 2030 is a robotic system that supports patients from the trunk to the feet and provides mobility to lower limbs and trunk stability. Likewise, it is the case of ReWalk, an exoskeleton that combines robotics and human assistance for people who have suffered spinal cord injury [18]. Although several patients have shown huge improvements in their daily life, these kinds of devices have been scarcely developed for children [19]. This shows a lack of socio-philosophical perspective during the definition of the design principles of wearable robotic exoskeletons for people with DMD, which should include a patient-based approach to increase the acceptance of exoskeletons, reduce the stigmatization, and deal with the dilemma of assistance and acceptance of the technology [20].

The control strategy implemented into a gait exoskeleton is a pivotal point in the successful acceptance of a wearable exoskeleton. Specifically, control strategies for gait assistant exoskeletons vary according to the therapy objectives or the patient's mobility disorder. In general, the control architectures of wearable exoskeletons are divided into three hierarchy levels: (1) a supervisory level, (2) an impedance control level, and (3) a position/torque control level [21]. The top level performs a supervisory activity that defines the control objectives. In this part of the control architecture, a finite state machine is commonly used to determine the controller's operation mode. These operation modes could be selected based on technologies that use manual command devices that work as a patient interface to the exoskeleton [22–24], bio-electrical signals that act as event-triggers with myoelectric signals or brain–computer interfaces [25,26], or motion and force sensors that identify movement intention [27,28].

The intermediate control level focuses on impedance control, which is devoted to the interaction between the exoskeleton and the patient. This control level looks to promote the active participation of the patient during therapy in such a way that the exoskeleton assists with motion as needed [29]. Although the impedance control could result in significant progress in the rehabilitation process, this is a technique not suitable for patients with low muscle strength. In these cases, low-level control takes special importance because it could impose a tracking control policy to follow a predefined trajectory. This activity has a strong influence on driving human motor learning by reinstating neuroplasticity and improving motor functions [30]. In this control level, feedback control strategies are used to guarantee that the exoskeleton performs motion along a predefined trajectory, which is generally adjusted by rehabilitation personnel according to the treatment required for each patient. Alternatively, nominal gaits of healthy people are used as a walking reference pattern. This reference pattern is adapted according to the interacting forces between the patient and exoskeleton to adjust the target trajectory and to adapt the gait pattern to the patient's needs [31]. This is the case of dynamic trajectory adjustments based on impedance control strategies [32]. Exhaustive reviews about control strategies used in assistance exoskeletons were presented in [33–35], where the use of predefined trajectories based on healthy people's gait was identified as a trend.

Considering the loss of muscular strength that DMD patients suffer, this paper proposes a tracking trajectory control strategy with predefined gait pattern, and a supervisory system to define the operation mode. Here, the operation mode selection depends on the contact conditions between the feet and the ground, which must be recognized with external sensors installed to identify the support leg and the motion intention [36].

This research carries out a mechatronic design of an exoskeleton to aid the lower limbs movement of children that have been affected by DMD. The main contribution of this research is the development of a nonlinear control strategy for the hybrid system formed by the exoskeleton and the child's body. The proposed controller is used in a simulated environment during therapy with children affected by DMD, where the controller is devoted to achieving trajectory tracking that ensure reliable therapy. These simulations provide evidence of the controller's robustness and performance. The remainder of this paper is organized as follows: Section 2.1 describes the mechatronic design of the exoskeleton. Section 2.2 presents the dynamic model of the hybrid system formed by the exoskeleton and child. Section 2.3 proposes a nonlinear control based on differential geometry tools to guarantee a trajectory tracking task. Section 3 contains the results of numerical evaluations of the exoskeleton in a simulated environment. Section 3.1 includes an analysis of the performance and robustness of the controller evaluated with parameters variation. Finally, Section 4 summarizes the accomplishments of this work and draws recommendations for future implementations.

2. Methods

2.1. Exoskeleton Design

Active exoskeletons are electromechanical devices built as augmentative systems that enhance the patient physical performance. The mechanical design of a gait exoskeleton considers the kinematic chain formed by the legs attached to the robotic system with a grounded pivot located at the hip joint [37]. In order to design a system to help children with DMD, it is considered the anthropometric data of Latin American children between the ages of five and eight years old [38]. Since a child's growth rate is approximately 6–7 cm and 3–3.5 kg per year [21], the dimensions are susceptible to high variability; therefore, the exoskeleton mechanisms are designed to be adaptable to each patient's needs. In order to make the exoskeleton suitable for a large range of patients, the mechanisms are designed with the anthropometric mean values shown in Table 1 and with extendable elements.

Table 1. Anthropometric measurements of Latin American children.

Anthropometric Measurements			
Body Section	**Type of Measure**	**Min. Size (mm)**	**Max. Size (mm)**
Hip	height width	74 229	102 255
Thigh	length width	276 74	387 102
Forefoot	length width	266 65	355 81
Foot	length width	170 64	213 76

Considering the variability of the anthropometric measurements, an adaptable mechanism is designed to fit each patient's requirements. In this way, Figure 1a shows a mechanism of nut-screw used to extend or shorten the length of the exoskeleton's thigh and forefoot. In the same way, a back support mechanism is designed using the assembly system shown in Figure 1b, which allows for a natural walking process considering the torso elevation and declination. One of the main challenges in orthopedic devices design is to find the appropriate attachment between the machine and the patient. In this design, the effects of misalignment between rotation axes of the exoskeleton and the patient legs are mitigated by using a motion transmission system that includes a magnetic brake, shown in Figure 1c, which is coupled to the flexible actuator shown in Figure 1d. The use of a series elastic actuator allows for minimizing energy consumption, reducing the required peak motor torque, and attenuating the impacts produced during leg support exchange in bipedal walking [39]. Recent designs of lower-limb exoskeletons have pointed out the benefits of using compliant mechanisms to offer the patients adaptability, safety, efficiency, and comfort [40]. The complaint mechanism used here is adapted from our previous work in the construction of a compliant knee orthosis for rehabilitation [41]. In this transmission system, the magnetic brake works complementary to the actuators to allow the locking of any joint at any time. This permits reconfiguration of the mechanism to a standing position without using the action of the motors, which results in reduced energy consumption. Figure 2 shows a lateral view of the exoskeleton assembly, which includes the distribution of the adjustable mechanisms, the actuators, brakes, and lumbar support.

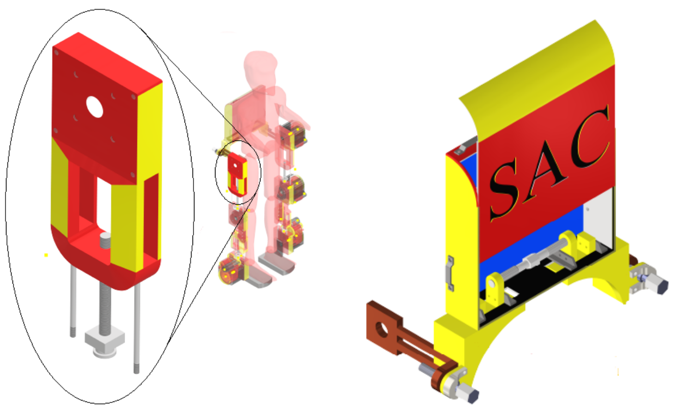

(**a**) Thigh mechanism (**b**) Back support mechanism

Figure 1. *Cont.*

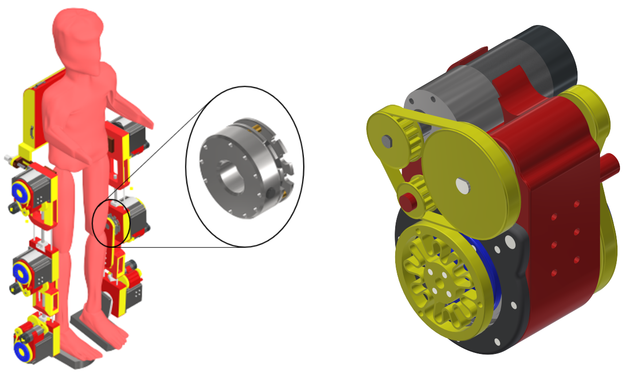

(**c**) Magnetic brake (**d**) Flexible serial actuator

Figure 1. Exoskeleton mechanisms.

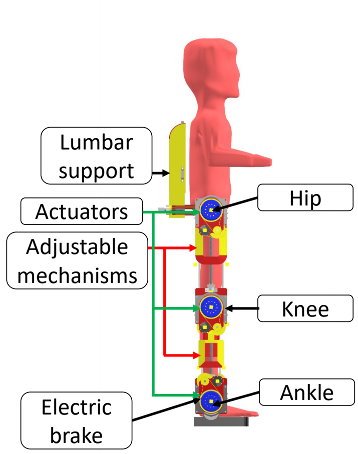

Figure 2. Exoskeleton main design.

2.2. Hybrid Dynamic Model of Exoskeleton and Child's Body

Since the exoskeleton is designed for children between five and eight years old [38], the kinematic chain formed by the child's body and the exoskeleton is computed to analyze the motion of a natural walking process, where the balance of the body must be kept and guided by the movement of the swing leg, while the support leg joints are locked by the electrical brakes. Figure 3 shows a kinematic model of the hybrid system, where the blue and red dots represent the limb center of masses and the joint positions, respectively.

In order to numerically simulate the dynamic behavior of the hybrid system formed by the child and exoskeleton, two dynamic models are built to reproduce the walking during the single support phase in the sagittal plane. The first model uses the Simscape Multibody software from Matlab®, which allows for modeling and simulating the multibody mechanical systems without extracting mathematical equations. This numerical model is used to test the control strategies in a relevant simulation environment. The second model is built using mathematical expressions that allow for designing a control strategy that ensures closed-loop stability.

Given the short time span of the double support in bipedal walking, the dynamics of this phase is neglected and considered as an instantaneous event [42]. Here, the same approach is used; therefore, the focus is on the single-support walking phase, where one leg is over the ground while the other leg is in forward motion. Thus, the mathematical model considers the swing leg as an open kinematic chain with three actuated degrees of freedom (DoF) and the support leg as an inverted pendulum with the joints locked by the electrical brakes and the contact between the support leg-end and the floor as a passive pivot. Even though the support leg has actuated joints, the idea of activating the brakes to impose motion restriction is proposed to reduce the torque requirements and energy consumption, leaving the support leg motion as a passive element.

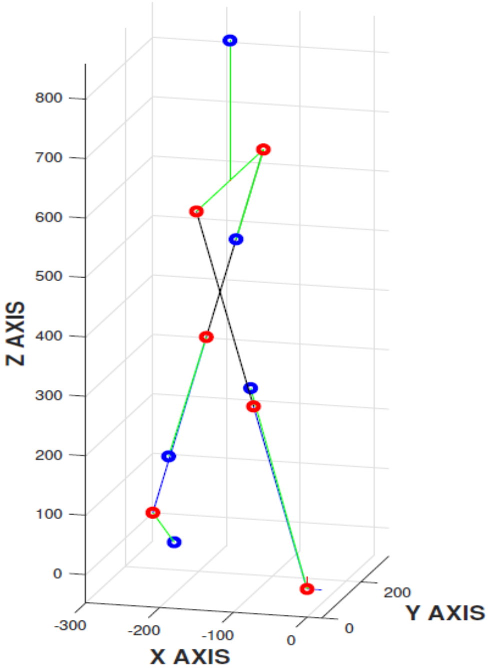

Figure 3. Kinematic model system.

Since the motion is analyzed in the sagittal plane, the Lagrange method is used to find the governing equation of the planar mechanism. In this scenario, the angular position of the swing leg's hip, knee, and ankle are defined, as shown in Figure 4, with the generalized coordinates $\mathbf{q} := [\theta_1\ \theta_2\ \theta_3]^T$, respectively. Those coordinates are used to define the Euler-Lagrange equation as follows:

$$D(\mathbf{q})\ddot{\mathbf{q}} + C(\mathbf{q}, \dot{\mathbf{q}})\dot{\mathbf{q}} + G(\mathbf{q}) = \tau, \quad (1)$$

where $D(\mathbf{q})$ is the inertial matrix; $C(\mathbf{q}, \dot{\mathbf{q}})$ is the matrix of Coriolis and centripetal forces; $G(\mathbf{q})$ is the matrix of gravitational effects; $\tau := [\tau_1\ \tau_2\ \tau_3]^T$ is the vector of external torques; and $\dot{\mathbf{q}}$ and $\ddot{\mathbf{q}}$ are the vectors of angular velocities and accelerations, respectively.

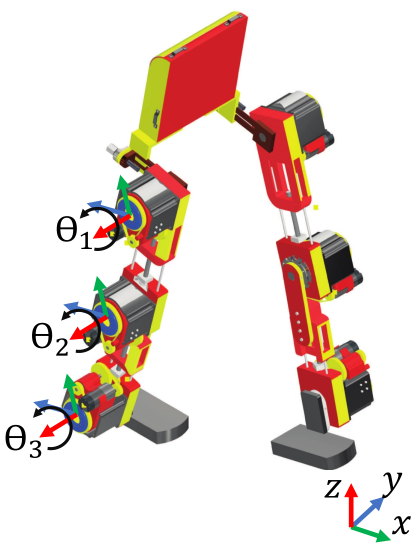

Figure 4. Generalized coordinate distribution.

To set a validation test, the natural and forced responses of the model are simulated using the body parameter shown in Table 2. First, the natural response is obtained by letting the mechanism be in its initial condition, different from the rest position, and by releasing it without torque input. The mechanism shows its natural behavior when approaching an equilibrium point, as shown in Figure 5a. This figure allows us to identify the resting position of the mechanism and shows the damping effect on the joint's behavior. The second validation test looks for a forced response. In this case, the mechanism with similar initial conditions to the previous test is exposed to a constant input torque of 2 Nm in each joint. The results of this simulation are shown in Figure 5b, where how the mechanism approaches a final position is visible, which is different than the resting position of the natural response. This test allows us to identify the control input gains, which are positive for the hip and knee joints and negative for the ankle.

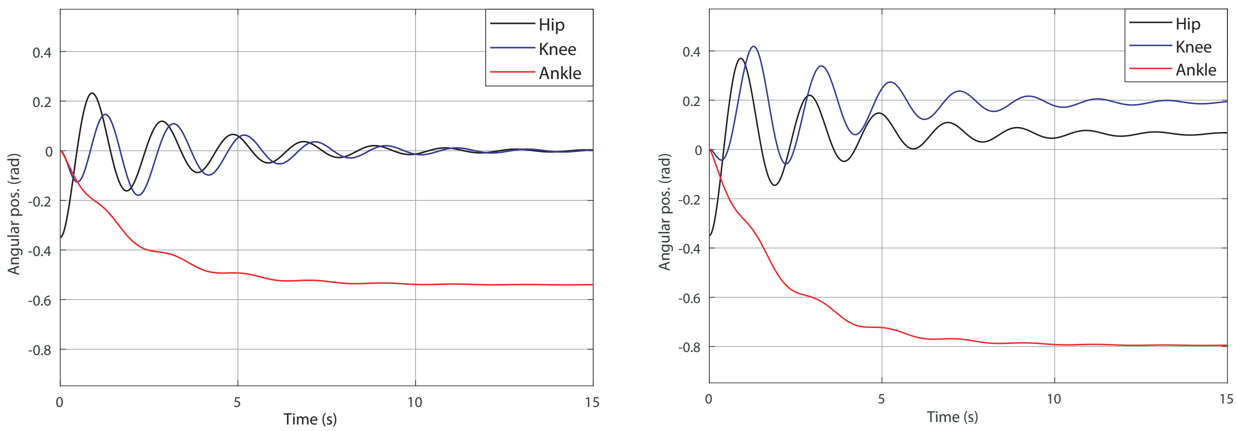

(**a**) Natural response (**b**) Forced response

Figure 5. Model validation tests.

Table 2. Physical body-exoskeleton design criteria.

Body Section	Mass (kg)	Inertia (kg·m^2)	Friction Coeff. (kg·m^2/s)	Center of Mass [X,Y,Z] (mm)
Fixed leg	11.12	1.120	0.8	[0, 0, 338]
Trunk	18.05	2.080	0.8	[0, 0, 235]
Thigh	7.46	0.138	0.8	[0, 0, 158]
Foreleg	3.66	0.031	0.8	[0, 0, 338]
Foot	0.89	0.002	0.8	[29, 67, 47]

2.3. Motion Control Strategy

The control architecture proposed in this paper includes a supervisory level and a trajectory tracking level. The complete motion control strategy is graphically described in Figure 6. In this control strategy, the supervisory level selects the operation mode, which in this case is a definition of which leg is supporting the body weight and which leg is swinging forward. This selection is executed based on the information from force sensors installed under the exoskeleton feet. After the roles of each leg are defined, the supervisory control activates the electrical brakes from the support leg and starts the tracking control in the swing leg. The tracking control is divided into a trajectory design task and a trajectory tracking control law. The trajectory design task is defined according to the medical treatment or therapy objectives. It could be a repetition of a prescribed isotonic exercise or even the execution of a normal gait. The tracking control law looks to ensure that the exoskeleton performs the assigned task in a safe way. This is a challenge that involves guaranteeing closed-loop stability under the parameter's uncertainty due to the variability related to the changing anthropometric measurements of each patient.

Each task involved in the exoskeleton's motion tracking control is further developed in the following sections.

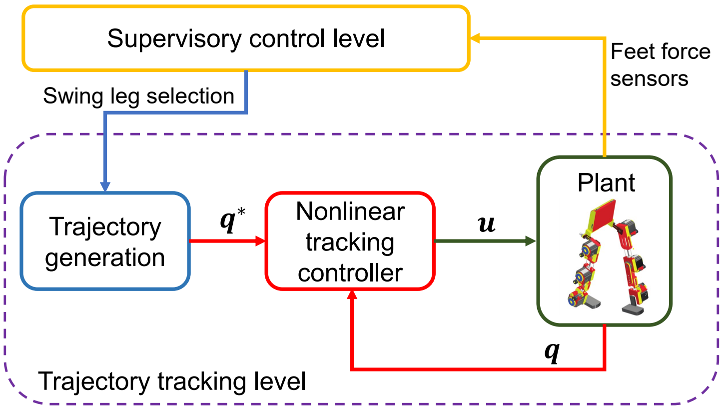

Figure 6. Motion control strategy.

2.3.1. Trajectory Design Based on Gait Parameters.

In physical therapy, the gait pattern is defined by the medical personnel and should be adapted to each patient's needs. Therefore, an adaptable trajectory generator is necessary to satisfy the flexibility required in an assistant exoskeleton. In this sense, a target trajectory for each joint is defined through the selection of the coefficients of smooth polynomials, which satisfy a set of kinematic constraints defined by the physician. To guarantee a smooth motion, the target trajectories are determined based on the mathematical structure of Bézier polynomials, which have bounded derivatives and allow us to define the trajectory as a function of the step time, T [43]. Then, the reference trajectories are given by the following:

$$q_j^*(s) = \sum_{i=0}^{M} \beta_{i,j} \frac{M!}{i!(M-i)!} s^i (1-s)^{M-i}, \quad j = 1,2,3, \tag{2}$$

where M is the polynomial degree; $\beta_{i,j}$ is the ith coefficient of the jth polynomial; and s is a transition variable with values between zero and one, both included. s is defined as follows:

$$s := \frac{t}{T},$$

where t is the elapsed time since the beginning of each step.

Based on the mathematical structure of the Bézier polynomials, a cost function is defined to minimize the torque required to perform the target trajectory. In this case, the cost function is defined as follows:

$$J(\beta) = \int_0^T \|\tau^*\|_2^2 dt, \tag{3}$$

where τ^* is the result of the inverse dynamics of (1), such as that

$$\tau^* = D(\mathbf{q}^*)\ddot{\mathbf{q}}^* + C(\mathbf{q}^*, \dot{\mathbf{q}}^*)\dot{\mathbf{q}}^* + G(\mathbf{q}^*), \tag{4}$$

where using (2), the position reference vector is defined as $\mathbf{q}^*(s) := [q_1^*(s)\ q_2^*(s)\ q_3^*(s)]^T$ and its first and second-time derivatives are defined as

$$\dot{\mathbf{q}}^*(s) = \frac{\partial \mathbf{q}^*(s)}{\partial s} \frac{ds}{dt}, \tag{5}$$

and

$$\ddot{\mathbf{q}}^*(s) = \frac{\partial \dot{\mathbf{q}}^*(s)}{\partial s} \frac{ds}{dt}, \tag{6}$$

respectively. Thus, the coefficients of the Bézier polynomials are selected by solving the optimization problem:

$$\begin{aligned} \text{find } \beta_{i,j}, \quad \forall\, i,j, \quad & \text{such that:} \\ \min \quad & J(\beta) \\ \text{subject to:} \quad & \text{dynamic constraints,} \\ & \text{kinematic constraints,} \\ & \text{safety constraints,} \end{aligned} \tag{7}$$

where the dynamic constraints include the exoskeleton and child's dynamics computed in (1), the kinematic constraints are selected according to the therapy conditions, and the safety constraints are set to prevent injuries due to over-elongation of the muscles or the transition through non-anatomical positions.

In order to evaluate the exoskeleton's motion control strategy, the kinematic constraints are defined to set a gait pattern, which uses as input parameters the step length, step angle, cadence, speed, and time of each step. Table 3 shows the parameters of a healthy person's gait, which are used to define a nominal gait pattern. Based on the defined gait parameters, a trajectory is planned to perform a forwarding motion, as shown in Figure 7. This trajectory considers a sagittal walking that ensures smooth motion through the imposition of initial and final velocities and accelerations equal to zero.

Table 3. Gait trajectory parameters [44] .

	Step Length (m)	**Step Angle (degrees)**	**Cadence (steps/min)**	**Speed (m/s)**	**Step Time (s)**
Value	0.68	[102 to 78]	20	0.226	3

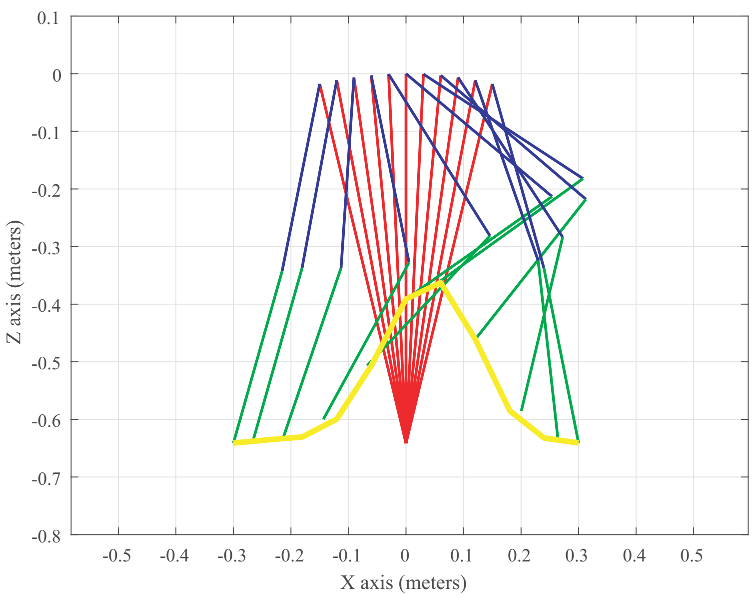

Figure 7. Evolution of the leg trajectory in the sagittal plane.

2.3.2. Nonlinear Tracking Control Strategy

In order to perform a stable and smooth motion, a nonlinear controller based on a feedback linearization strategy is designed [45]. Using the Euler–Lagrange Equation (1), the nonlinear model is presented in an input affine state space representation as follows:

$$\dot{\mathbf{x}} = \mathbf{f}(\mathbf{x}) + \mathbf{g}(\mathbf{x})\mathbf{u}, \tag{8}$$

where $\mathbf{x} := \begin{bmatrix} \mathbf{q} \\ \dot{\mathbf{q}} \end{bmatrix}$ is the state vector, $\mathbf{u} := \begin{bmatrix} \tau_1 \\ \tau_2 \\ \tau_3 \end{bmatrix}$ is the vector of control inputs,

$$\mathbf{f}(\mathbf{x}) = \begin{bmatrix} \dot{\mathbf{q}} \\ D^{-1}(\mathbf{q})[-C(\mathbf{q}, \dot{\mathbf{q}})\dot{\mathbf{q}} - G(\mathbf{q})] \end{bmatrix}, \tag{9}$$

and

$$\mathbf{g}(\mathbf{x}) = \begin{bmatrix} 0 \\ D^{-1}(\mathbf{q}) \end{bmatrix}. \tag{10}$$

Based on the model (8), the control output is defined as follows:

$$\mathbf{y} := \mathbf{h}(\mathbf{x}) = \mathbf{q} - \mathbf{q}^*, \tag{11}$$

where $\mathbf{q}^*$ is the reference trajectory computed in Section 2.3.1.

To find a mathematical form that expresses the output vector as a function of the control-input vector, successive time differentiations of (11) were performed until the vector of control-input signals is explicit. Since the trajectory references are designed to be smooth, their time derivatives are negligible. Then, the time differentiation result is

$$\begin{aligned} \frac{d\mathbf{y}}{dt} &= \frac{\partial \mathbf{h}(\mathbf{x})}{\partial \mathbf{x}}\dot{\mathbf{x}}, &(12)\\ &= \begin{bmatrix} \frac{\partial \mathbf{h}(\mathbf{x})}{\partial \mathbf{q}} & \frac{\partial \mathbf{h}(\mathbf{x})}{\partial \dot{\mathbf{q}}} \end{bmatrix}[\mathbf{f}(\mathbf{x}) + \mathbf{g}(\mathbf{x})\mathbf{u}], &(13)\\ &= \nabla\mathbf{h}(\mathbf{x})\mathbf{f}(\mathbf{x}) + \nabla\mathbf{h}(\mathbf{x})\mathbf{g}(\mathbf{x})\mathbf{u}, &(14)\\ &= L_f\mathbf{h} + L_g\mathbf{h}\mathbf{u}, &(15) \end{aligned}$$

where $\nabla\mathbf{h}(\mathbf{x})$ is the gradient of $\mathbf{h}(\mathbf{x})$, and $L_f\mathbf{h}$ and $L_g\mathbf{h}$ are the Lie derivatives of $\mathbf{h}(\mathbf{x})$ along $\mathbf{f}(\mathbf{x})$ and $\mathbf{g}(\mathbf{x})$, respectively. Given that $L_g\mathbf{h}\mathbf{u}$ is equal to zero, the first time-derivative of the output is independent of the control input; therefore, the second derivative is necessary. This is,

$$\begin{aligned} \frac{d^2\mathbf{y}}{dt^2} &= \begin{bmatrix} \frac{\partial}{\partial \mathbf{q}}\left(\frac{\partial \mathbf{h}(\mathbf{x})}{\partial \mathbf{q}}\dot{\mathbf{q}}\right) & \frac{\partial \mathbf{h}}{\partial \mathbf{q}} \end{bmatrix}[\mathbf{f}(\mathbf{x}) + \mathbf{g}(\mathbf{x})\mathbf{u}], &(16)\\ &= L_f^2\mathbf{h} + L_gL_f\mathbf{h}\mathbf{u}, &(17) \end{aligned}$$

where $L_f^2\mathbf{h}$ is the second Lie derivative of $\mathbf{h}(\mathbf{x})$ along $\mathbf{f}(\mathbf{x})$ and $L_gL_f\mathbf{h}$ is a decoupling term that is locally invertible around the operation region [46].

Considering the local transformation in (17), a feedback linearization control law is defined as follows:

$$\mathbf{u} = L_gL_f\mathbf{h}^{-1}\left(-L_f^2\mathbf{h} + \mu\right), \tag{18}$$

with μ being an auxiliary control signal to be specified. Applying the control law (18) to (17), the resulting dynamics

$$\frac{d^2\mathbf{y}}{dt^2} = \mu, \tag{19}$$

are shown to be linear. However, the stability of (19) is unknown. To guaranty a stable behavior, μ is defined as

$$\mu := -K_d\frac{d\mathbf{y}}{dt} - K_p\mathbf{y}, \tag{20}$$

where K_d and K_p are diagonal matrices used as control gains, which are selected to be strictly positive. This results in a Hurwitz system with the form:

$$\frac{d^2\mathbf{y}}{dt^2} + K_d\frac{d\mathbf{y}}{dt} + K_p\mathbf{y} = 0, \tag{21}$$

which is asymptotically stable.

3. Results

3.1. Numerical Analysis

In order to evaluate the performance and robustness of the nonlinear controller, two numerical simulations were carried out over a relevant simulation environment. These simulations reproduced the physical conditions of a rehabilitation therapy room. The selected controller's gains are

$$K_p = \begin{bmatrix} 18 & 0 & 0 \\ 0 & 18 & 0 \\ 0 & 0 & 18 \end{bmatrix} \quad \text{and} \quad \begin{bmatrix} 80 & 0 & 0 \\ 0 & 80 & 0 \\ 0 & 0 & 80 \end{bmatrix}.$$

The first simulation considers the evaluation of the hybrid system under nominal conditions during a step with the swing leg tracking the precomputed trajectory and the support leg locked with a unactuated pivot between the support foot and the floor. The evolution of motion is shown in Figure 8, where it is possible to identify satisfactory trajectory tracking with bonded control signals. The performance of the controller is quantified with the integral square of the error (ISE) and with the integral square of the control signal (ISU), which are defined as follows:

$$ISE := \int_0^{t_f} \mathbf{e}^T \mathbf{e} \, dt, \tag{22}$$

$$ISU := \int_0^{t_f} \mathbf{u}^T \mathbf{u} \, dt, \tag{23}$$

where $\mathbf{e}$ is the vector of tracking errors, defined as

$$\mathbf{e} := \begin{bmatrix} \theta_1 - \theta_1^* \\ \theta_2 - \theta_2^* \\ \theta_3 - \theta_3^* \end{bmatrix},$$

and t_f is the evaluation period of time, which in this case corresponds to three seconds.

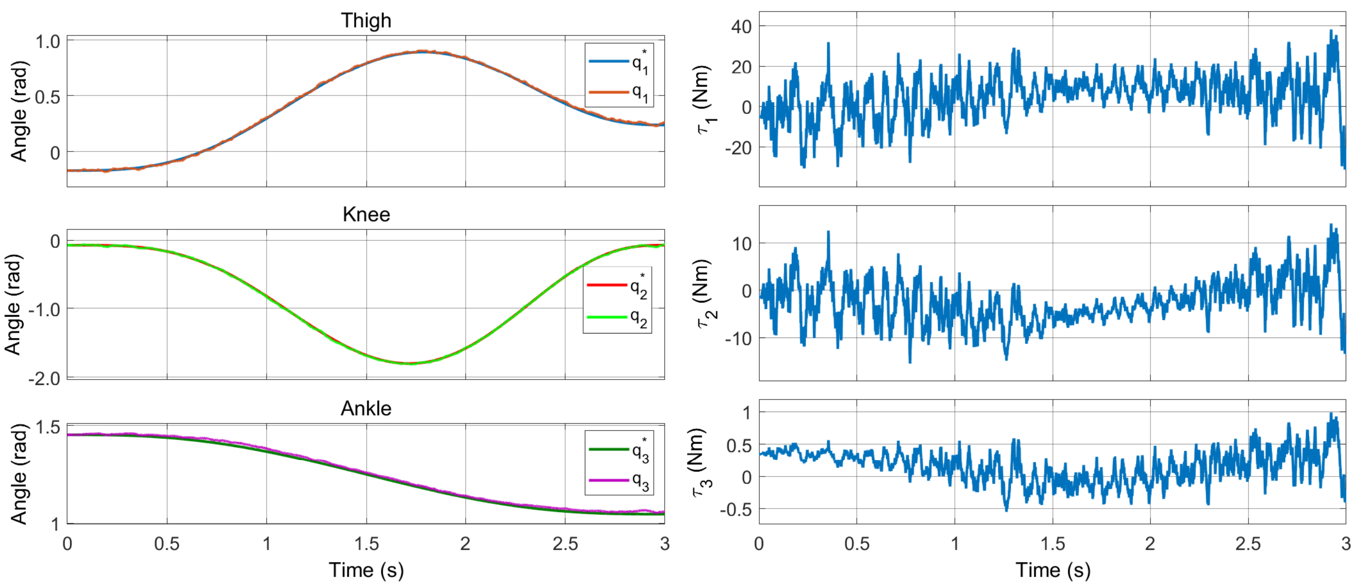

Figure 8. Nonlinear control for trajectory tracking.

The second simulation test evaluated the controller robustness against parameter variation, which is a typical case in the use of exoskeletons with different patients or with the same patient over an extended period of time. In this case, the nonlinear control was evaluated with variation in the patient's masses. With this purpose, nine simulations were conducted with numerical models of children with masses between 80% and 120% from the nominal mass values. Figure 9 shows the system behavior in each simulation scenario with an envelope that bound all the deviations from the nominal behavior, which confirms the controller robustness against parameter uncertainties. The performance indexes, ISE and ISU, of the evaluations with parameter variation are shown in Figure 10. This figure highlights the deviation of the indexes from the nominal value, which allows for measuring the performance degradation with respect to parameter variation. The worst-case scenario was compared with the nominal behavior in Table 4, where the performance indexes of both simulations, nominal and parameter variation, are registered. The difference between these indexes is irrelevant, resulting in a controller whose performance is not substantially degraded by variations in the children's anthropometric parameters.

Table 4. Performance indexes.

Index	ISE	ISU
Nominal conditions	0.00056	36,725
Variation of parameters	0.00077	37,336

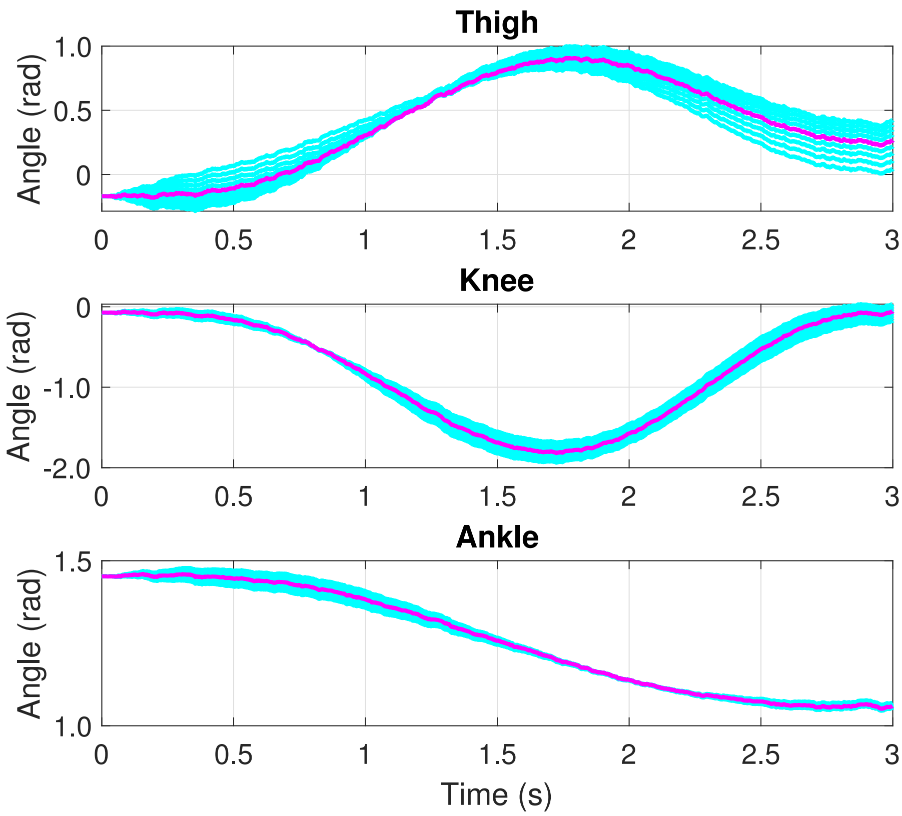

Figure 9. Nonlinear control robustness test against parameter variation. (Nominal behavior: central line, parameters variation: shadow.)

In order to develop a visual inspection of the motion evolution during walking therapy, a virtual scenario was designed, which reproduced the therapy environment. As shown in Figure 11, the virtual scenario is used to evaluate the exoskeleton during a single-support walking phase. This simulation shows stable walking, with the exoskeleton performing a smooth evolution of motion (https://youtu.be/z5kDJDO2Wuk).

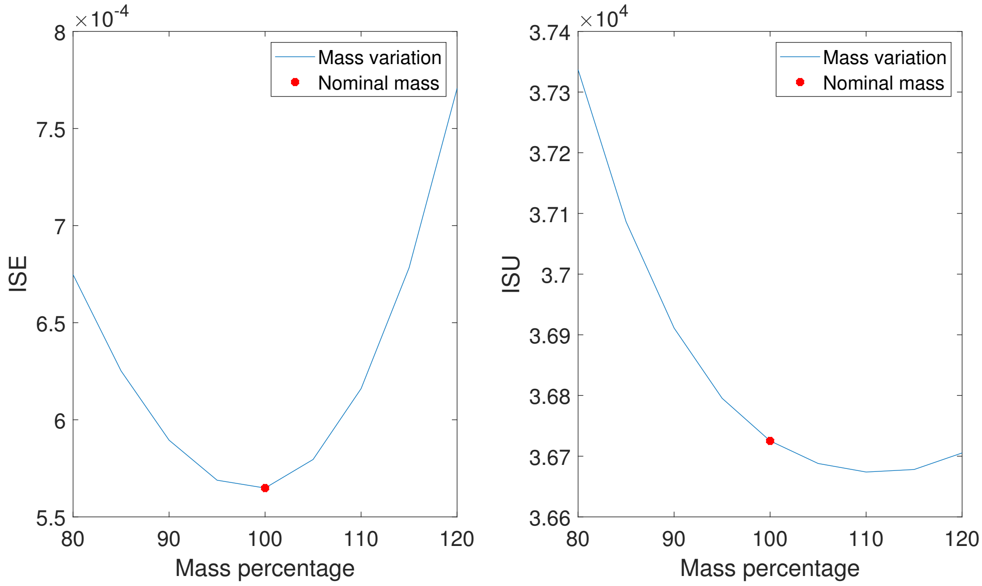

Figure 10. Robustness and performance indexes with parameter variation.

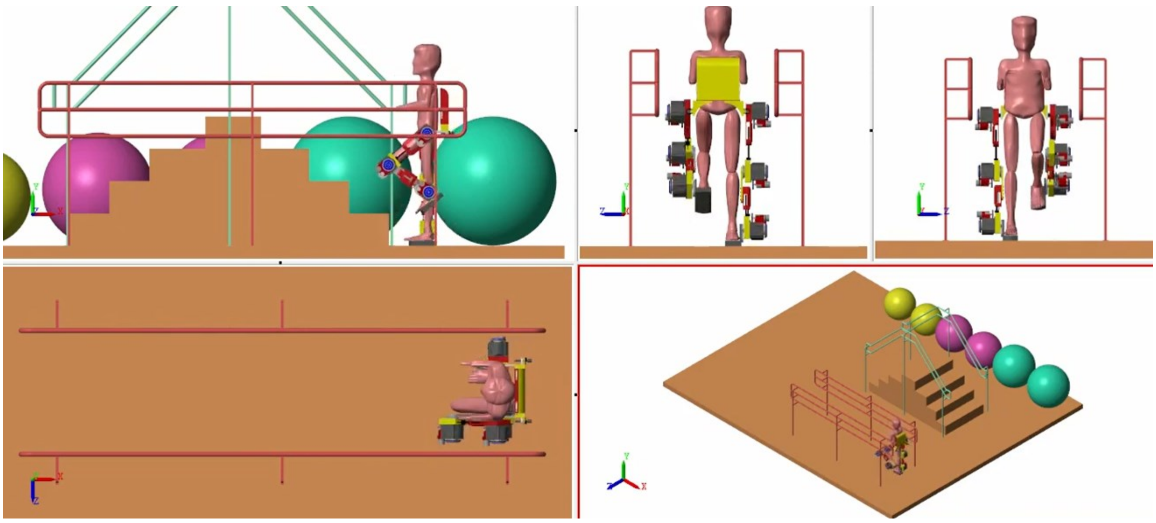

Figure 11. Virtual scenario for walking rehabilitation.

4. Conclusions

A mechatronics design approach was used to develop a gait-assistance exoskeleton for therapy in children with Duchenne muscular dystrophy. This exoskeleton aims to increase the autonomy of patients with advanced muscular dystrophy. In this way, an adaptable mechanism was designed to fit the requirements of patients, and a nonlinear control strategy was designed to assist with gait control by tracking predefined trajectories. The proposed controller was evaluated in a virtual scenario under nominal operation conditions with the body parameters of a six-year-old child. The controller's robustness and performance were computed using indexes to quantify the integral square error and the integral square control signal. These evaluations showed evidence of an effective performance of the nonlinear control under uncertain conditions.

The nonlinear controller evaluations showed evidence of a robust performance during the trajectory-tracking control task, which confirms that feedback linearization based on differential geometry transformation is a suitable methodology to design feedback-control strategies for gait-assistance exoskeletons. Future implementation of the proposed nonlinear control technique should consider the external disturbances produced by the interaction between the patient and the exoskeleton. Although these interactions are bounded loads, they could reduce the performance of the controller or saturate the motor actuators.

Author Contributions: Conceptualization, J.A.-L.; methodology, J.A.-L.; software, D.T., F.V., H.R. and A.P.; validation, D.T., F.V., H.R. and A.P.; formal analysis, J.A.-L., D.T., and Á.G.; investigation, J.A.-L., F.V., H.R. and A.P.; resources, J.A.-L. and Á.G.; writing—original draft preparation, J.A.-L., D.T. and Á.G.; writing—review and editing, J.A.-L., D.T. and Á.G.; visualization, J.A.-L.; supervision, J.A.-L., D.T. and Á.G. All authors have read and agreed to the published version of the manuscript.

Funding: The first author was supported by the European Union under the plan Next Generation EU and by the Spanish *Ministerio de Universidades* under RD 289/2021.

Institutional Review Board Statement: Not applicable

Informed Consent Statement: Not applicable

Acknowledgments: European Union for the plan Next Generation EU and the Spanish *Ministerio de Universidades*.

Conflicts of Interest: The authors declare no conflicts of interest. The funders had no role in the design of the study; in the collection, analyses, or interpretation of data; in the writing of the manuscript; or in the decision to publish the results.

References

1. Mendell, J.R.; Lloyd-Puryear, M. Report of MDA muscle disease symposium on newborn screening for Duchenne muscular dystrophy. *Muscle Nerve* **2013**, *48*, 21–26.
2. Mah, J.K.; Korngut, L.; Dykeman, J.; Day, L.; Pringsheim, T.; Jette, N. A systematic review and meta-analysis on the epidemiology of Duchenne and Becker muscular dystrophy. *Neuromuscul. Disord.* **2014**, *24*, 482–491.
3. Baiardini, I.; Minetti, C.; Bonifacino, S.; Porcu, A.; Klersy, K.; Petralia, P.; Balestracci, S.; Tarchino, F.; Parodi, S.; Canonica, W.; et al. Quality of life in Duchenne Muscular Dystrophy: The subjective Impact on Children and Parents. *J. Child Neurol.* **2011**, *26*, 707–713.
4. Schofield, C.and Evans, K.; Young, H.; Paguinto, S.G.; Carroll, K.; Townsend, E.; Downs, J. The development of a consensus statement for the prescription of powered wheelchair standing devices in Duchenne muscular dystrophy. *Disabil. Rehabil.* **2020**, *44*, 1889–1897.
5. Biggar, W.; Politano, V.; Passamano, J.; Alman, B.; Palladino, A.; Comi, L.; Nigro. Deflazacort in Duchenne muscular dystrophy: A comparison of two different protocols. *Neuromuscul. Disord.* **2004**, *14*, 476–482.
6. Soto Vargas, J. Distrofia Muscular de Duchenne. Reporte de un caso. *Revista Médica MD* **2010**, *2*, 33.
7. Osorio, A.N.; Cantillo, J.M.; Salas, A.C.; Garrido, M.M.; Padilla, J.V. Consensus on the diagnosis, treatment and follow-up of patients with Duchenne muscular dystrophy. *Neurol. (Engl. Ed.)* **2019**, *34*, 469–481.
8. Brooke, M.; Fenichel, G.; Griggs, R.; Mendell, J.; Moxley, R.; Florence, J.; King, W.; Pandya, S.; Robison, J.; Schierbecker, J.; et al. Duchenne muscular dystrophy: Patterns of clinical progression and effects of supportive therapy. *Neurology* **1989**, *39*, 475–475.
9. Banala, S.; Hun Kim, S.; Agrawal, S.; Scholz, J. Robot assisted gait training with active led exoskeleton (ALEX). *IEEE Trans. Neural Syst. Rehabil. Eng.* **2009**, *17*, 2–8.
10. Kooren, P.N.; Lobo-Prat, J.; Keemink, A.Q.; Janssen, M.M.; Stienen, A.H.; de Groot, I.J.; Paalman, M.I.; Verdaasdonk, R.; Koopman, B.F. Design and control of the Active A-Gear: A wearable 5 DOF arm exoskeleton for adults with Duchenne muscular dystrophy. In Proceedings of the 2016 6th IEEE International Conference on Biomedical Robotics and Biomechatronics (BioRob), Singapore, 26–29 June 2016; pp. 637–642.
11. Nizamis, K.; Stienen, A.H.; Kamper, D.G.; Keller, T.; Plettenburg, D.H.; Rouse, E.J.; Farina, D.; Koopman, B.F.; Sartori, M. Transferrable expertise from bionic arms to robotic exoskeletons: perspectives for stroke and duchenne muscular dystrophy. *IEEE Trans. Med. Robot. Bionics* **2019**, *1*, 88–96.
12. Schabron, B.; Desai, J.; Yihun, Y. Wheelchair-mounted upper limb robotic exoskeleton with adaptive controller for activities of daily living. *Sensors* **2021**, *21*, 5738.
13. Estilow, T.; Glanzman, A.M.; Powers, K.; Moll, A.; Flickinger, J.; Medne, L.; Tennekoon, G.; Yum, S.W. Use of the Wilmington robotic exoskeleton to improve upper extremity function in patients with Duchenne muscular dystrophy. *Am. J. Occup. Ther.* **2018**, *72*, 7202345010p1–7202345010p5.
14. Bakker, J.; De Groot, I.; Beckerman, H.t.a.; De Jong, B.; Lankhorst, G. The effects of knee-ankle-foot orthoses in the treatment of Duchenne muscular dystrophy: Review of the literature. *Clin. Rehabil.* **2000**, *14*, 343–359.
15. Case, L.E.; Apkon, S.D.; Eagle, M.; Gulyas, A.; Juel, L.; Matthews, D.; Newton, R.A.; Posselt, H.F. Rehabilitation management of the patient with Duchenne muscular dystrophy. *Pediatrics* **2018**, *142*, S17–S33.

16. Bushby, K.; Finkel, R.; Birnkrant, D.J.; Case, L.E.; Clemens, P.R.; Cripe, L.; Kaul, A.; Kinnett, K.; McDonald, C.; Pandya, S.; et al. Diagnosis and management of Duchenne muscular dystrophy, part 2: implementation of multidisciplinary care. *Lancet Neurol.* **2010**, *9*, 177–189.
17. Romero, P.; Palomino-Díaz, V.; Delgado-Oleas, G.; Gutiérrez, A.; Martín, C.; Martín, I.; Rocon, E. Diseño y modelo de un robot actuado por cables para ayudar a caminar a niños con parálisis cerebral. In Proceedings of the XII Simposio CEA de Bioingeniería, Madrid, España, 3 June 2021.
18. Zeilig, G.; Weingarden, H.; Zwecker, M.; Dudkiewicz, I.; Bloch, A.; Esquenazi, A. Safety and tolerance of the ReWALK exoskeleton suit for ambulation by people with complete spinal cord injury: A pilot study. *J. Spinal Cord Med.* **2012**, 35, 96–101.
19. Dijsseldonk, R.V.; Rijken, H.; Nes, I.V.; van de Meent, H.; Keijsers, N. Predictors of exoskeleton motor learning in spinal cord injured patients. *Disabil. Rehabil.* **2019**, *43*, 1982–1988.
20. Kapeller, A.; Nagenborg, M.H.; Nizamis, K. Wearable robotic exoskeletons: A socio-philosophical perspective on Duchenne muscular dystrophy research. *Paladyn J. Behav. Robot.* **2020**, *11*, 404–413.
21. Sarajchi, M.; Al-Hares, M.K.; Sirlantzis, K. Wearable Lower-Limb Exoskeleton for Children With Cerebral Palsy: A Systematic Review of Mechanical Design, Actuation Type, Control Strategy, and Clinical Evaluation. *IEEE Trans. Neural Syst. Rehabil. Eng.* **2021**, *29*, 2695–2720.
22. Chen, B.; Zhong, C.H.; Zhao, X.; Ma, H.; Qin, L.; Liao, W.H. Reference joint trajectories generation of CUHK-EXO exoskeleton for system balance in walking assistance. *IEEE Access* **2019**, *7*, 33809–33821.
23. Chen, B.; Zhong, C.H.; Zhao, X.; Ma, H.; Guan, X.; Li, X.; Liang, F.Y.; Cheng, J.C.Y.; Qin, L.; Law, S.W.; et al. A wearable exoskeleton suit for motion assistance to paralysed patients. *J. Orthop. Transl.* **2017**, *11*, 7–18.
24. Schrade, S.O.; Dätwyler, K.; Stücheli, M.; Studer, K.; Türk, D.A.; Meboldt, M.; Gassert, R.; Lambercy, O. Development of VariLeg, an exoskeleton with variable stiffness actuation: First results and user evaluation from the CYBATHLON 2016. *J. Neuroeng. Rehabil.* **2018**, *15*, 1–18.
25. Wang, C.; Wu, X.; Wang, Z.; Ma, Y. Implementation of a brain-computer interface on a lower-limb exoskeleton. *IEEE Access* **2018**, *6*, 38524–38534.
26. Colucci, A.; Vermehren, M.; Cavallo, A.; Angerhöfer, C.; Peekhaus, N.; Zollo, L.; Kim, W.S.; Paik, N.J.; Soekadar, S.R. Brain–Computer Interface-Controlled Exoskeletons in Clinical Neurorehabilitation: Ready or Not? *Neurorehabilit. Neural Repair* **2022**, *36*, 15459683221138751. https://doi.org/10.1177/15459683221138751.
27. Hua, Y.; Fan, J.; Liu, G.; Zhang, X.; Lai, M.; Li, M.; Zheng, T.; Zhang, G.; Zhao, J.; Zhu, Y. A novel weight-bearing lower limb exoskeleton based on motion intention prediction and locomotion state identification. *IEEE Access* **2019**, *7*, 37620–37638.
28. Zhu, L.; Wang, Z.; Ning, Z.; Zhang, Y.; Liu, Y.; Cao, W.; Wu, X.; Chen, C. A novel motion intention recognition approach for soft exoskeleton via IMU. *Electronics* **2020**, *9*, 2176.
29. Aguirre-Ollinger, G.; Colgate, J.E.; Peshkin, M.A.; Goswami, A. Active-impedance control of a lower-limb assistive exoskeleton. In Proceedings of the 2007 IEEE 10th international conference on rehabilitation robotics, Noordwijk, The Netherlands, 13–15 June 2007; pp. 188–195.
30. Hussain, S.; Xie, S.Q.; Liu, G. Robot assisted treadmill training: Mechanisms and training strategies. *Med. Eng. Phys.* **2011**, *33*, 527–533.
31. Bortole, M.; Del Ama, A.; Rocon, E.; Moreno, J.C.; Brunetti, F.; Pons, J.L. A robotic exoskeleton for overground gait rehabilitation. In Proceedings of the 2013 IEEE International Conference on Robotics and Automation, Karlsruhe, Germany, 6–10 May 2013; pp. 3356–3361.
32. Chen, L.; Wang, C.; Song, X.; Wang, J.; Zhang, T.; Li, X. Dynamic trajectory adjustment of lower limb exoskeleton in swing phase based on impedance control strategy. *Proc. Inst. Mech. Eng. Part J. Syst. Control. Eng.* **2020**, *234*, 1120–1132.
33. Tucker, M.R.; Olivier, J.; Pagel, A.; Bleuler, H.; Bouri, M.; Lambercy, O.; Millán, J.d.R.; Riener, R.; Vallery, H.; Gassert, R. Control strategies for active lower extremity prosthetics and orthotics: A review. *J. Neuroeng. Rehabil.* **2015**, *12*, 1–30.
34. Yan, T.; Cempini, M.; Oddo, C.M.; Vitiello, N. Review of assistive strategies in powered lower-limb orthoses and exoskeletons. *Robot. Auton. Syst.* **2015**, *64*, 120–136.
35. Baud, R.; Manzoori, A.R.; Ijspeert, A.; Bouri, M. Review of control strategies for lower-limb exoskeletons to assist gait. *J. Neuroeng. Rehabil.* **2021**, *18*, 1–34.
36. Young, A.J.; Ferris, D.P. State of the art and future directions for lower limb robotic exoskeletons. *IEEE Trans. Neural Syst. Rehabil. Eng.* **2016**, *25*, 171–182.
37. Pérez, Y.S.C.; Passeiro, O. Diseño preliminar de la estructura mecánica de un exoesqueleto para la rehabilitación de la marcha humana. In Proceedings of the VIII Conferencia Cietífica Internacional de Ingeniería Mecánica, Pasto, Colombia, 17 nov 2014; Volume 1, pp. 1–11.
38. Avila, R.; Prado, L.; Gonzalez, E. *Dimensiones Antropométricas de la Población Latinoamericana: Mexico, Cuba, Colombia, Chile*; Universidad de Guadalajara: Guadalajara, Mexico, 2007.
39. Nieto, E.A.B.; Rezazadeh, S.; Gregg, R.D. Minimizing energy consumption and peak power of series elastic actuators: A convex optimization framework for elastic element design. *IEEE/ASME Trans. Mechatronics* **2019**, *24*, 1334–1345.
40. Sanchez-Villamañan, M.d.C.; Gonzalez-Vargas, J.; Torricelli, D.; Moreno, J.C.; Pons, J.L. Compliant lower limb exoskeletons: A comprehensive review on mechanical design principles. *J. Neuroeng. Rehabil.* **2019**, *16*, 1–16.

41. Cortés-Orjuela Sergio, C.C.R.; Torres, D.; Arcos-Legarda, J. Mechatronic Design of a Compliant Knee Orthosis for Rehabilitation. In Proceedings of the X Congreso Internacional de Ingeniería Mecatrónica y Automatización, Barranquilla, Colombia, 5–7 May 2021; pp. 1–8.
42. Arcos-Legarda, J.; Cortes-Romero, J.; Tovar, A. Robust compound control of dynamic bipedal robots. *Mechatronics* **2019**, *59*, 154–167.
43. Arcos-Legarda, J.; Calderon-Diaz, M. Optimal Trajectory Planning with Dynamic Obstacles Avoidance for Mobile Robots Navigation. In Proceedings of the International Conference on Advanced Engineering Theory and Applications, Bogotá, Colombia, 6–8 November 2019; Springer: Berlin/Heidelberg, Germany, 2019; pp. 639–648.
44. Ordoñez, R.; Karam, M. *Frecuencia de las Alteraciones de la Marcha en Niños de 6–10 Años Obtenidas Mediante la Aplicación de un Análisis Cuantitativo de los Parámetros Espacio-Temporales en Estudiantes de 4º a 6º del Turno Matutino de la Escuela Primaria José Guadalupe Victoria, Lerma estado de Mexico, Durante el Periodo de mayo—Junio de 2012*; Universidad autónoma del estado de México: Toluca de Lerdo, Mexico, 2014.
45. Guillard, H.; Bourles, H. Robust feedback linearization. In Proceedings of the 14th International Symposium on Mathematical Theory of Networks and Systems, Perpignan, France, 19–23 June 2000.
46. Isidori, A. *Nonlinear Control Systems: An Introduction*; Springer: Berlin/Heidelberg, Germany, 1985.